Eur Biophys J (2007) 36:491–498
DOI 10.1007/s00249-006-0119-x

ARTICLE

Membrane binding of a lipidated N-Ras protein studied in lipid monolayers

Frank Bringezu · Monika Majerowicz · Shaoying Wen · Guido Reuther · Kui-Thong Tan · Jürgen Kuhlmann · Herbert Waldmann · Daniel Huster

Received: 6 September 2006 / Revised: 23 November 2006 / Accepted: 28 November 2006 / Published online: 22 December 2006

Abstract The adsorption of doubly lipidated full-length N-Ras protein on 1,2-dipalmitoyl-*sn*-phosphatidylcholine (DPPC) monolayers was studied by lateral pressure analysis, grazing incidence X-ray diffraction (GIXD), and specular reflectivity (XR). N-Ras protein adsorbs to the DPPC monolayer (lateral pressure of 20 mN/m) from the subphase thereby increasing the lateral pressure in the monolayer by 4 mN/m. The protein insertion does not alter the tilt angle and structure of the lipid molecules at the air/water interface but influences the electron density profile of the monolayer. Further, electron density differences into the subphase were observed. The Fresnel normalized reflectivity could be reconstructed in the analysis using box models yielding electron density profiles of the DPPC monolayer in the absence and in the presence of N-Ras protein. The electron density profiles of the DPPC monolayer in the presence of Ras showed clear intensity variations in the headgroup/glycerol/upper chain region, the so-called interface region where previous bilayer studies had confirmed Ras binding.

Dedicated to Prof. K. Arnold on the occasion of his 65th birthday.

F. Bringezu (✉) · M. Majerowicz · S. Wen
Institute of Medical Physics and Biophysics,
University of Leipzig, Härtelstrasse 16-18,
04107 Leipzig, Germany
e-mail: frank.bringezu@medizin.uni-leipzig.de

G. Reuther · D. Huster
Junior Research Group "Structural Biology of Membrane Proteins", Institute of Biotechnology,
Martin Luther University Halle-Wittenberg,
Kurt-Mothes-Str. 3, 06120 Halle, Germany

K.-T. Tan · J. Kuhlmann · H. Waldmann
Max Planck Institute of Molecular Physiology,
Otto-Hahn-Str. 11, 44227 Dortmund, Germany

Introduction

The regulation of cellular functions is controlled by intracellular protein cascades that transmit external signals via transmembrane receptors to the cell nucleus. Several membrane-associated and soluble proteins are involved in this regulation of the signal transmission process (Hancock et al. 1990, 1991; Reuther and Der 2000). A frequently encountered feature of membrane-associated proteins involved in signal transduction is their post-translational lipid modification, which provides them with sufficient hydrophobic character for association with the cellular membrane (Casey 1995). A typical example for such a lipid-modified signaling protein is the membrane bound GTPase Ras. Ras proteins are mediators in the cell signal cascade from the receptor tyrosine kinases to the cellular nucleus that activate downstream effectors to stimulate cell proliferation and differentiation. Failure of these regulators can lead to an uncontrolled cell growth and finally cancer. Mutated forms of the Ras protein have been found in more than 30% of all human cancers (Wittinghofer and Waldmann 2000). Membrane binding is essential for the function of all members of the Ras family, which carry either one, two, or three lipid anchors that insert into the membrane (Wittinghofer and Waldmann 2000). Non-lipid-modified Ras proteins are cytosolic and consequently inactive (Dudler and Gelb 1996). Here we study the insertion of the human N-Ras protein into lipid monolayers. The N-Ras protein

that is subject of the current study is farnesylated at the C-terminal recognition region (Cys186) and palmitoylated at Cys181.

The lipid bilayer of biological membranes can be viewed as two weakly coupled monolayers. Consequently, Langmuir monolayers represent interesting model systems mimicing a membrane surface (Parker 1990; Giehl et al. 1999; Seitz et al. 1999). Such systems exhibit interesting ordering phenomena on the mesoscopic length scale that can be studied with molecular resolution by means of grazing incidence X-ray diffraction (GIXD) (Helm et al. 1987; Als-Nielsen and Möhwald 1991; Als-Nielsen et al. 1994; Spaar et al. 2004; Maltseva and Brezesinski 2004) and specular reflectivity (XR) (Helm et al. 1987; Als-Nielsen et al. 1994; Malkova et al. 2005) as well as spectroscopic (Dluhy and Cornell 1985; Flach et al. 1994) and optical (Hénon and Meunier 1991; McConnell 2006) methods. In particular, adsorption phenomena have successfully been reported on these systems. Since monolayers reflect half of a membrane, they are rather limited for the study of trans-membrane processes or structural features, but they offer relevant models to study processes at the lipid/water interface of the membrane (Brezesinski and Möhwald 2003). This offers the possibility to modify the density of the lipids at the interface in a defined way and alter other physicochemical parameters (e.g. molecular area, lateral pressure, temperature, subphase composition etc.). Unlike diffraction (Nagle and Tristram-Nagle 2000) or solid-state NMR techniques (Huster 2005), monolayer measurements are not compromised by restriction of the water content, which make them superior techniques to study protein adsorption phenomena.

Previous solid-state NMR, neutron diffraction, fluorescence, and ATR FTIR measurements have contributed to suggest an atomistic model of membrane binding of Ras proteins (Schroeder et al. 1997; Huster et al. 2001, 2003; Vogel et al. 2005; Reuther et al. 2006a, b). According to theses studies, the protein backbone of the C-terminus of lipid modified N-Ras protein is located in the lipid/water interface of the membrane, while the hydrophobic side chains and lipid modifications insert into the hydrophobic core of the membrane. This structural ensemble is characterized by intense molecular dynamics similar to what has been known from pure phospholipid membranes. In addition, recent work on Ras has revealed the partitioning of the lipidated protein into liquid disordered membrane domains (Janosch et al. 2004; Nicolini et al. 2006). Finally, in a pioneering monolayer study, the insertion of Ras proteins into lipid monolayers and their orientation on the lipid surface were determined (Meister et al. 2006).

In this study we have examined the binding of the lipidated N-Ras protein to dipalmitoylphosphatidylcholine (DPPC) Langmuir monolayers at the air/liquid interface. The chain length of DPPC closely matches the length of the lipid anchor region of the N-Ras protein thus providing a suitable hydrophobic environment for Ras insertion. To obtain information on the Ras adsorption and the in-plane structure on a molecular scale, both GIXD and XR measurements were conducted.

Materials and methods

Materials

1,2-Dipalmitoyl-*sn*-glycero-3-phosphatidylcholine (DPPC) was purchased from Avanti Polar Lipids (Alabaster, AL; purity >99%) and used without further purification. Lipid solutions of a concentration of about 1 mM were prepared using chloroform and methanol. The protein stock solution in buffer (10 mM Hepes, 10 mM NaCl, 1 mM $MgCl_2$, pH 7.4) was used for the injection of N-Ras into the subphase of the monolayer to allow protein adsorption. The monolayer experiments were carried out on a Hepes buffer subphase (10 mM Hepes, 10 mM NaCl, 1 mM $MgCl_2$, pH 7.4) at a temperature of 20°C. All aqueous solutions were prepared using Milli-Q deionized water of a specific electrical resistivity of >18 MΩcm.

The synthesis of the farnesylated and hexadecylated N-Ras lipopeptide was described before (Bader et al. 2000; Volkert et al. 2003). Briefly, C terminally truncated wildtype N-Ras (residues 1–181) was expressed in *E. coli* CK600K and purified via DEAE ion exchange chromatography and gel filtration. Coupling with N-Ras lipopeptides was performed in stoichiometric amounts in 20 mM Tris/HCl, pH 7.4, 5 mM $MgCl_2$ supplemented with the detergent Triton X114. The detergent allowed for convenient separation of lipoprotein product and truncated educt after completion of the coupling reaction. After removal of Triton X114 from the N-Ras lipoprotein by another DEAE ion exchange chromatography, the lipoprotein was concentrated and adjusted to 20 mM Tris/HCl, pH 7.4, 5 mM $MgCl_2$, 2 mM DTE by size exclusion filtration in Amicon® concentrators. All protein batches were analyzed by SDS-PAGE and MALDI-TOF mass spectrometry.

X-ray reflectivity on monolayers

The surface pressure area isotherms were collected using a Langmuir film balance (Riegler & Kirstein,

Potsdam, Germany) with a Teflon trough equipped with a Wilhelmy type pressure sensor and a single moveable Teflon barrier that allows compression and expansion of the monolayers by changing the area. Monolayers were obtained after spreading a certain volume from the stock solution on the subphase and subsequent equilibration for about 10 min. The isotherms were recorded at a compression speed of about 4 Å^2/molecule/min. For the lipoprotein adsorption study the protein was injected underneath the lipid monolayer through the air/water interface at a constant lateral pressure using a Hamilton syringe.

Grazing incidence X-ray diffraction (GIXD) and specular X-ray reflectivity measurements (XR) were performed using the liquid surface diffractometer at the beamline BW1 (HASYLAB, DESY, Hamburg, Germany) (Kjaer et al. 1989; Frahm et al. 1995). The beamline features a temperature controlled Langmuir through in a sealed container mounted on a vibration damped Huber table. During the experiments, the experimental box containing the trough was filled with helium atmosphere to reduce the interfering scattering from the air. The synchrotron beam was made monochromatic by a Beryllium (002) crystal. Specular reflectivity was measured as a function of the vertical exit angle, α_i that equals the exit angle, α_f, of the reflected X-rays. The experiments where performed between $0.5\alpha_c < \alpha_{i/f} < 35\alpha_c$ with α_c being the critical angle on water at the given wavelength, $\alpha_c = 0.13°$. The reflected signal was recorded using a NaI scintillation counter.

For the analysis of the XR data, we employed a two step procedure. In the first step the model independent algorithm of Hamley and Pedersen (Hamley and Pedersen 1994; Pedersen and Hamley 1994), based on a constrained least square optimization of B-spline functions that define the relevant electron density fluctuations along the interface normal was used to get a profile function describing the reflectivity data. As expected, the profiles obtained resemble those of a layered structure at the interface. In a second step the electron density profile is modeled by a stack of homogeneous slabs ("boxes"), each being characterized by a height of constant electron density. The electron density profile is obtained by convolution of the step function with a Gaussian function accounting for the roughness at the boundaries due to thermal excitation and atomic roughness at the interfaces between the slabs (Braslau et al. 1985). This function is fitted to the result obtained in a model independent algorithm (first step) to get a molecular description of the monolayer. From the data, the total volume of each box and the number of electrons can be calculated taking the area per molecule from the isotherm measurements into account. Given the number of electrons in the lipid headgroup, the extra electrons obtained can be associated with bound water molecules.

GIXD experiments were performed at an angle of incidence of $0.85*\alpha_c$ (α_c is the critical angle for total external reflection). A linear position sensitive detector (PSD) (OED-100-M, Braun, Garching, Germany) with a vertical acceptance $0 < Q_z < 1.27$ Å^{-1} was used for recording the diffracted intensity as a function of both the vertical (Q_z) and the horizontal (Q_{xy}) scattering vector components. The horizontal resolution of $Q_{xy} = 0.008$ Å^{-1} was determined by a Soller collimator mounted in front of the PSD. The analysis of the in-plane diffraction data yields lattice parameters of the crystalline part of the monolayer. The Q_{xy} peak positions yield lattice spacings according to $d_{hk} = 2\pi/Q_{xy}^{hk}$ from the 2D-lattice of the alkyl chains. The peak width, corrected by instrumental resolution, provides information about the coherence length L_{xy} along the reciprocal scattering vector Q_{xy}. The analysis of the out-of-plane scattering vector components along Q_z allows deriving information about the tilt angle and the tilt direction. For this analysis, the lipid chains are modeled by a cylinder of constant electron density. For more information about the principles of GIXD for the study of 2D crystalline films at the air/liquid interface, we kindly refer to detailed reviews found in the literature (Parker 1990; Jacquemain et al. 1991; Als-Nielsen et al. 1994; Kaganer et al. 1999).

Results and discussion

The effect of N-Ras binding to DPPC monolayers was studied via isotherm measurements. Figure 1 depicts the compression isotherm of a DPPC monolayer on a buffer subphase at 20°C. The pure lipid shows the typical coexistence region between a disordered liquid expanded phase and an ordered liquid condensed or solid phase (McConnell 2006). The transition pressure observed at 20°C amounts to ~4 mN/m. To prove for the monolayer insertion capabilities, the N-Ras protein was injected into the subphase underneath the lipid monolayer at 40 mN/m, to give a final lipid/protein molar ratio of 100:1. After 5 min of equilibration, the monolayer was expanded to 20 mN/m and the pressure was recorded as a function of time at constant area per lipid molecule (see insert of Fig. 1). After a long adsorption time of about 4.5 h, the pressure increase $\Delta\pi = \pi_2 - \pi_1$ of about 4 mN/m was observed, indicating the adsorption of the protein. Recompression of the film shows slightly larger area values per lipid molecule

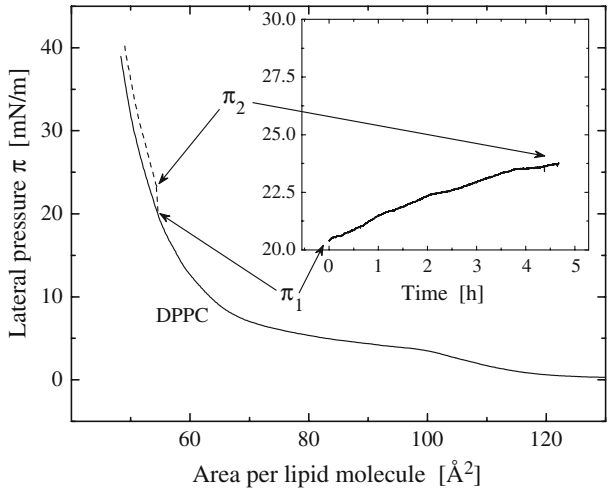

Fig. 1 Compression isotherm of DPPC on Hepes buffer (10 mM Hepes, 10 mM NaCl, 1 mM $MgCl_2$, pH 7.4) at 20°C before (*solid line*) and after (*dashed line*) injection of N-Ras into the subphase and subsequent adsorption of the protein to the lipid monolayer. The pressure versus time curve obtained after injection shown in the inset leads to a pressure increase of about 4 mN/m starting from the initial pressure

suggesting a partial incorporation of the protein. Ras protein incorporation into monolayers at a lower lateral pressure of 10 mN/m was also reported before (Meister et al. 2006).

The protein adsorption was performed at pressures clearly above the two-phase coexistence region of the lipid monolayer, thus under these conditions the pure lipid exhibits a liquid/condensed phase. Therefore, it was of great interest to study the condensed lipid structures using GIXD and the influence of the Ras adsorption on structural parameters. The experiments were performed at the same experimental condition as for the isotherm measurements, but GIXD is only sensitive for the crystalline domains of the monolayers, while in the isotherms the total area is given as sum of condensed film and defects. Figure 2 depicts selected contour plots of the X-ray diffraction intensities of DPPC on a buffer subphase before (left) and after (right) protein injection. The contour plots show the distribution of scattering intensity as a function of the in-plane scattering vector components Q_{xy} and the out-of-plane scattering vector component Q_z at different lateral pressures. The pure lipid shows three low-order diffraction peaks indicating an oblique chain lattice with the hydrophobic chains tilted in non-symmetry direction as also found previously on water. From the peak positions the tilt angle and 2D lattice spacings can be calculated (see Table 1). On increasing pressure, the peak positions shift to larger Q_{xy} and smaller Q_z values indicating a decrease of both, the 2D spacings of the chain lattice and the tilt of the chains from the surface normal. However, the oblique phase with strongly tilted chains remains present up to highest pressure investigated. At 40 mN/m, the width of the fitted Bragg rods gives a molecular length of about 22.8 Å. The diffraction pattern observed after N-Ras adsorption is shown in Fig. 2 (right). Again, three diffraction peaks are present in the whole pressure region. Neither Bragg peak positions nor the full width at half maximum values were affected by the presence of the protein (see Table 1). However, the intensities of the Bragg peaks extracted from the 2D diffraction patterns are slightly lower, suggesting that the protein is inserting into the monolayer, thus the number of condensed lipids in the footprint of the beam is decreased. The structure of the remaining condensed lipid domains is on the other hand not affected indicating that either the protein is excluded from the condensed domains or the insertion of the lipid anchor from the protein into the hydrophobic core must take place without changing the condensed DPPC lattice. These findings are supported by ^{2}H NMR studies on lipid bilayers (Huster et al. 2003; Vogel et al. 2005) and FTIR measurements on lipid monolayers (Meister et al. 2006) that show Ras protein insertion does not significantly affect the structural parameters of the lipids in bi- or monolayers, respectively.

In addition, the insertion of the protein into the monolayer would alter the electron density profile across the monolayer and into the aqueous phase. To prove the insertion of Ras into DPPC monolayers, we carried out X-ray reflectivity studies to gain information about the electron density distribution along the surface normal. The XR measurements were carried out for the pure monolayer and for the DPPC/N-Ras system after the adsorption at 24 mN/m and subsequent recompression at 40 mN/m. Figure 3a shows the Fresnel normalized reflectivity for DPPC and the model independent fit of the data at 24 and 40 mN/m. The analysis of the electron density profile obtained in the model independent fit is shown in Fig. 3b. For this analysis a two-box model was fitted to the calculated profile: one box representing the headgroup region and one for the tail region of the lipid molecule. The final result is obtained by the convolution of the step function with a Gaussian function to contribute for the roughness at the interface (Table 2). In order to limit the number of fitting parameters, the electron number in the tail region was fixed to 242 and the molecular area was set to the experimental value during the refinement. For the pure lipid monolayer at 24 mN/m, the total thickness of the film amounts to 23 Å, with hydrophobic and polar regions of 15.8 and 7.2 Å,

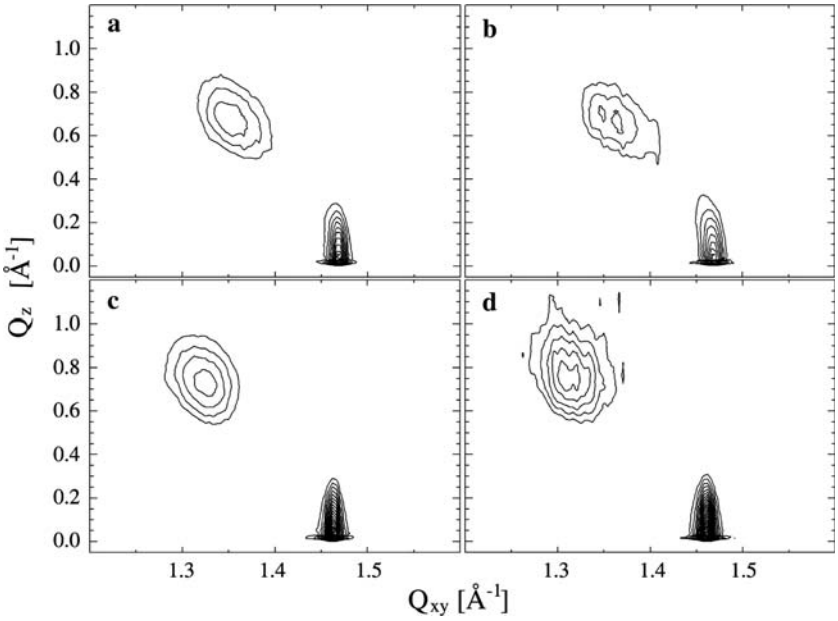

Fig. 2 Contour plots of the corrected X-ray intensities as function of Q_{xy} and Q_z for DPPC on Hepes buffer (10 mM Hepes, 10 mM NaCl, 1 mM $MgCl_2$, pH 7.4) (**a**, **c**) and DPPC with injected N-Ras protein (protein/lipid 1:100) (**b**, **d**) at 24 (**c**, **d**) and 40 mN/m (**a**, **b**)

Table 1 Best fit values of the in-plane (Q_{xy}) and out-of-plane (Q_z) scattering vector components, tilt angle (t), distortion of the unit cell from the hexagonal symmetry (ξ), tilt direction (ψ) and projected area per hydrocarbon chain of DPPC on buffer (10 mM Hepes, 10 mM NaCl, 1 mM $MgCl_2$, pH 7.4) at 20°C

π (mN/m)	Q_{xy} (ΔQ_{xy}) in (Å^{-1})			Q_z (ΔQ_z) in (Å^{-1})			ξ	t (°)	Tilt direction (ψ)	A_{xy} (Å^2)
DPPC on Hepes subphase										
24	1.46 (0.013)	1.33 (0.058)	1.31 (0.063)	0.03 (0.28)	0.73 (0.29)	0.76 (0.29)	0.14	34.0	21.2° from NN, oblique	24.4
30	1.46 (0.016)	1.35 (0.073)	1.33 (0.064)	0.04 (0.28)	0.69 (0.29)	0.73 (0.29)	0.12	32.4	19.9° from NN, oblique	24.0
40	1.47 (0.015)	1.36 (0.052)	1.34 (0.07)	0.05 (0.27)	0.65 (0.28)	0.70 (0.28)	0.11	30.8	18.9° from NN, oblique	23.6
DPPC on Hepes subphase, N-Ras injected										
24	1.46 (0.013)	1.33 (0.049)	1.31 (0.049)	0.03 (0.27)	0.73 (0.27)	0.76 (0.27)	0.14	34.2	21.0° from NN, oblique	24.6
40	1.47 (0.015)	1.38 (0.075)	1.35 (0.078)	0.04 (0.27)	0.66 (0.28)	0.70 (0.28)	0.10	30.8	18.9° from NN, oblique	23.4

respectively. The thickness of the slabs increases with pressure and at 40 mN/m 16.7 and 7.5 Å are obtained. From the slab representing the chain region the tilt can be calculated, which gives 34° and 29° at 24 and 40 mN/m, respectively. Both values are consistent with the data obtained in the GIXD measurements. Calculating the number of electrons contributing to headgroups gives larger values than expected from the chemical structure, thus providing the amount of water bound to the lipid headgroups. Assuming that the volumes of water and lipid headgroup are additive, the volume of the lipid headgroup (V_0) can easily be calculated taking the partial volume of one water molecule of about 30 Å^3 into account. The data obtained show that the V_0 values do not change significantly, instead changes in the headgroup hydration on compression must be assumed. It should be noted that a more detailed analysis of XR data for DPPC, separating the lipid headgroup into its components and using volume restricted distribution functions for the model description in combination with infrared and neutron reflectivity data (Schalke and Lösche 2000) yielded a similar pressure dependence of the headgroup hydration (Dyck et al. 2005).

Figure 4 depicts the comparison of the reflectivity data obtained before and after adsorption of N-Ras to DPPC monolayers at 24 mN/m lateral pressure (a) and the profiles obtained in the parameter free fit (b). The comparison of the profiles clearly indicates that both, the head group and the chain region of DPPC are influenced by the protein adsorption. As only small electron density contrast between water and protein must be assumed, a protein sub-layer bound to the lipid headgroups is difficult to detect, although it is likely to exist. The largest contrast difference in this system is expected between the lipid headgroups and the protein, while the contrast between chain region and protein and in particular the protein lipid anchor is rather small. This should particularly manifest in the headgroup/glycerol region of the monolayer, where Ras was shown to insert into lipid bilayers (Huster et al. 2001, 2003). This is reflected in the density profile comparison

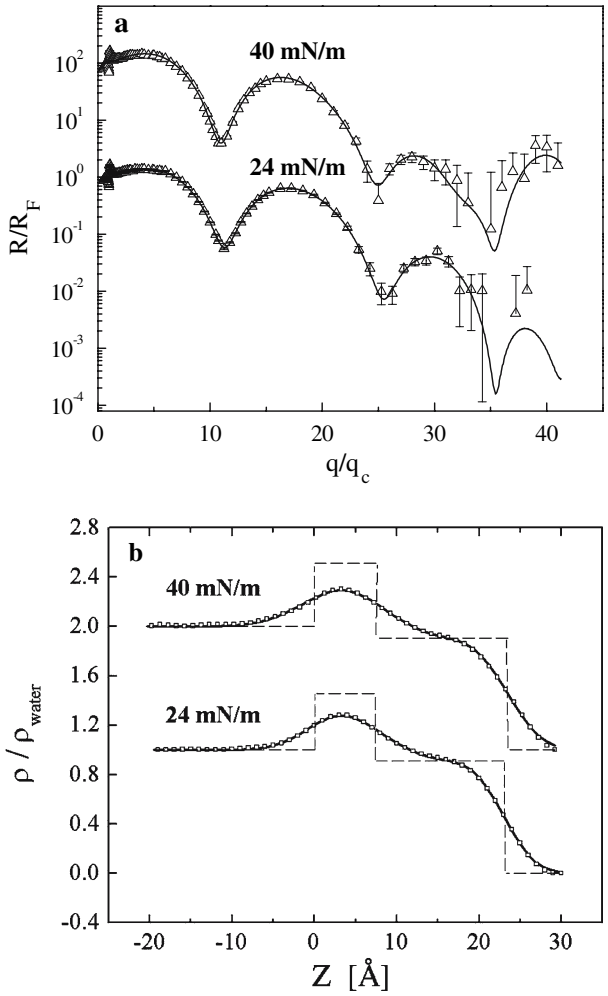

Fig. 3 **a** Fresnel normalized XR data for DPPC on Hepes buffer (10 mM Hepes, 10 mM NaCl, 1 mM $MgCl_2$, pH 7.4) and the fit result (*solid lines*) of the parameter free description of the experimental data obtained at 24 and 40 mN/m, respectively. **b** The fitted electron density profiles (*solid line*) corresponding to the parameter free description (*dots*) along with the fitted two-box models; one box describing the lipid head groups and one box for the tail regions

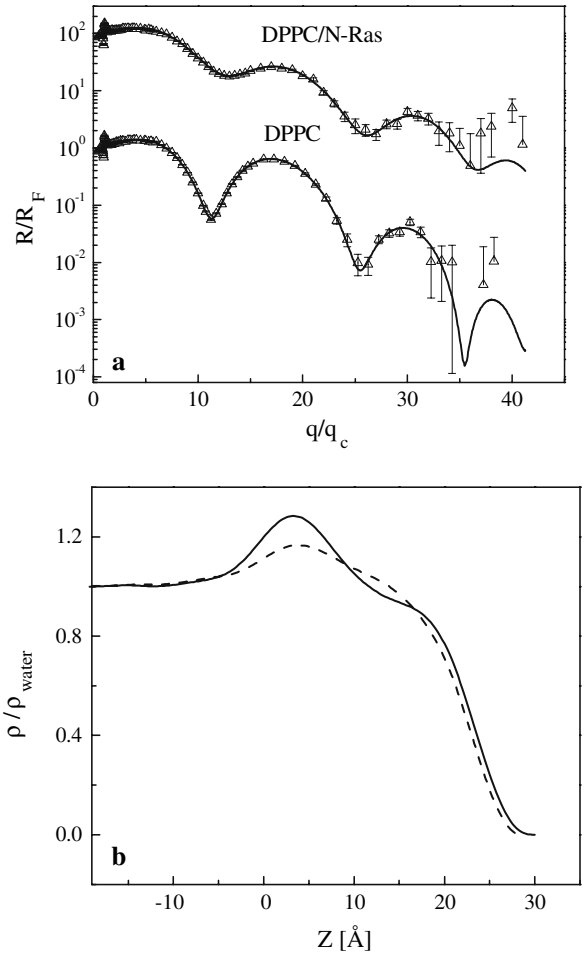

Fig. 4 **a** Fresnel normalized XR data for DPPC on Hepes buffer and the fit result (*solid lines*) of the parameter free description of the experimental data obtained at 24 mN/m before and after N-ras adsorption. The lower panel **b** compares the electron density profiles obtained from the parameter free description of the XR data for pure DPPC (*solid line*) and DPPC/N-Ras (*dashed line*)

showing largest deviations in the polar region of DPPC. In addition, limited insertion into the hydrophobic chain region is also evident. For the description of the profile obtained after adsorption of N-Ras we employed a three box model; one box accounting for the headgroup modified by the inserted protein anchor, the protein anchor inserting into the hydrophobic region of the lipid layer and the remaining part of the lipid chains (see Table 3; Fig. 5). In this description, the headgroup thickness remains constant, and the sum of both chain contributions roughly gives the dimensions of the chain slab obtained for the pure lipid. The reduction of the electron density in the headgroup slab can be explained by dilution of the headgroups either due

Table 2 Structural parameters for DPPC on buffer (10 mM Hepes, 10 mM NaCl, 1 mM $MgCl_2$, pH 7.4) at 20°C at different lateral pressures derived from X-ray reflectivity data

π (mN/m)	Headgroup region				Tail region		σ (Å)
	Δz (Å)	ρ/ρ_{water} (No. of e^-)	N_{water}	$V_{0,\,head}$	Δz (Å)	ρ/ρ_{water} (No. of e^-)	
24	7.2	1.46 (190)	2.6	310	15.8	0.91 (242*)	3.5
40	7.5	1.51 (176)	1.2	300	16.7	0.90 (242*)	4.1

Table 3 Structural parameters for DPPC on Hepes buffer (10 mM Hepes, 10 mM NaCl, 1 mM $MgCl_2$, pH 7.4) at 20°C after adsorption of N-Ras injected at 40 mN/m derived from X-ray reflectivity data

π (mN/m)	Box	Thickness L (Å)	Electron density (ρ/ρ_{water})	Roughness σ (Å)
24	Tail	7.2	0.90	3.3
	Tail + N-Ras	7.4	1.02	
	Head + N-Ras	7.5	1.25	

to insertion of the N-Ras lipid chains or by partial insertion of the protein. However, the increased electron density in the tail slab connected to the headgroup cannot be explained only by the insertion of the two Ras chains, since they have about the same electron density than the lipid chains from DPPC. Therefore, a partial incorporation of the protein with an anchor section must be assumed. This protein anchor adsorbs to the lipid headgroups and penetrates into the lipid chain region with a total depth of penetration of 14.9 Å. This insertion creates free space in the monolayer that needs to be filled by the hydrophobic chains, either by cooperative tilting of the lipid molecules or by insertion of the lipid chains connected to the protein. Given the results from the GIXD measurements that showed no alteration of the chain lattice, the increased space in the headgroup region must be compensated by the insertion of the hydrophobic chains from the Ras protein into the hydrophobic membrane core, thereby stabilizing the protein at the interface. Indeed, for Ras binding to lipid bilayers, a number of techniques have shown that the backbone of the C-terminus of lipid

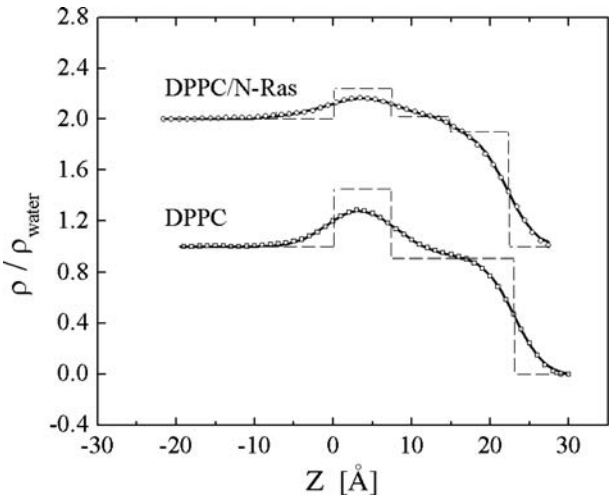

Fig. 5 The electron density profiles corresponding to the parameter free description of the XR data (*dots*) are shown with the fitted profile (*solid lines*) using a two-box model for the pure lipid and a three box model for the DPPC/N-Ras system (see text for details)

modified Ras is located in the lipid water interface of the membrane, while the lipid modifications and the hydrophobic side chains of the protein deeply insert into the hydrophobic core of the membrane (Huster et al. 2001, 2003).

On increasing lateral pressure at 40 mN/m, the reflectivity data obtained for the DPPC/N-Ras system are within experimental errors the same as found for the pure lipid (data not shown), suggesting a squeeze-out of the protein from the monolayer as also reported before (Meister et al. 2006). It should be noted, that this large pressure value is above the lateral pressure assumed to be relevant for lipid bilayers (Blume 1979). Therefore, we conclude that the insertion of the C-terminal region of N-Ras into DPPC under in vivo pressure conditions is a crucial event being essential for the function of the signal transduction.

Acknowledgments This study was supported by the Deutsche Forschungsgemeinschaft (HU 720/5-2, BR 1826/2-3).

References

Als-Nielsen J, Jaquemain D, Kjaer K, Lahav M, Levellier F, Leiserowitz L (1994) Principles and applications of grazing incindence X-ray and neutron scattering from ordered molecular monolayers at the air–water interface. Phys Rep 246:251–313

Als-Nielsen J, Möhwald H (1991) Synchrotron X-ray scattering studies of langmuir films. Elsevier, Amsterdam, pp 1–53

Bader B, Kuhn K, Owen DJ, Waldmann H, Wittinghofer A, Kuhlmann J (2000) Bioorganic synthesis of lipid-modified proteins for the study of signal transduction. Nature 403:223–226

Blume A (1979) A comparative study of the phase transitions of phospholipid bilayers and monolayers. Biochim Biophys Acta 557:32–44

Braslau A, Deutsch M, Pershan PS, Weiss AH, Als-Nielsen J, Bohr J (1985) Surface roughness of water measured by X-ray reflectivity. Phys Rev Lett 54:114–117

Brezesinski G, Möhwald H (2003) Langmuir monolayers to study interactions at model membrane surfaces. Adv Colloid Interface Sci 100–102:563–584

Casey PJ (1995) Protein lipidation in cell signaling. Science 268:221–225

Dluhy RA, Cornell DG (1985) In situ measurement of the infrared spectra of insoluble monolayers at the air–water interface. J Phys Chem 89:3195–3197

Dudler T, Gelb MH (1996) Palmitoylation of Ha-Ras facilitates membrane binding, activation of downstream effectors, and meiotic maturation in *Xenopus* oocytes. J Biol Chem 271:11541–11547

Dyck M, Krüger P, Lösche M (2005) Headgroup organization and hydration of methylated phosphatidylethanolamines in Langmuir monolayers. Phys Chem Chem Phys 7:150–156

Flach CR, Brauner JW, Taylor JW, Baldwin RC, Mendelsohn R (1994) External reflection FTIR of peptide monolayer films in situ at the air/water interface: experimental design, spectra-structure correlations, and effects of hydrogen–deuterium exchange. Biophys J 67:402–410

Frahm R, Weigelt J, Meyer G, Materlik G (1995) X-ray undulator beamline BW1 at Doris III. Rev Sci Instrum 66:1677–1680

Giehl A, Lemm T, Bartelsen O, Sandhoff K, Blume A (1999) Interaction of the GM2-activator protein with phospholipid-ganglioside bilayer membranes and with monolayers at the air–water interface. Eur J Biochem 261:650–658

Hamley WI, Pedersen JS (1994) Analysis of neutron and X-ray reflectivity data. I. Theory. J Appl Cryst 27:29–35

Hancock JF, Paterson H, Marshall CJ (1990) A polybasic domain or palmitoylation is required in addition to the CAAX motif to localize p21ras to the plasma membrane. Cell 63:133–139

Hancock JF, Cadwallader K, Paterson H, Marshall CJ (1991) A CAAX or a CAAL motif and a second signal are sufficient for plasma membrane targeting of Ras proteins. EMBO J 10:4033–4039

Helm CA, Möhwald H, Kjaer K, Als-Nielsen J (1987) Phospholipid monolayer density distribution perpendicular to the water surface. A synchrotron X-ray reflectivity study. Europhys Lett 4:697–703

Hénon S, Meunier J (1991) Microscopy at the brewster angle: direct observation of first order phase transitions in monolayers. Rev Sci Instrum 62:963–969

Huster D (2005) Investigations of the structure and dynamics of membrane-associated peptides by magic angle spinning NMR. Prog Nucl Magn Reson Spectrosc 46:79–107

Huster D, Kuhn K, Kadereit D, Waldmann H, Arnold K (2001) High resolution magic angle spinning NMR for the investigation of a Ras lipopeptide in a lipid bilayer. Angew Chem Int Ed 40:1056–1058

Huster D, Vogel A, Katzka C, Scheidt HA, Binder H, Dante S, Gutberlet T, Zschörnig O, Waldmann H, Arnold K (2003) Membrane insertion of a lipidated Ras peptide studied by FTIR, solid-state NMR, and neutron diffraction spectroscopy. J Am Chem Soc 125:4070–4079

Jacquemain D, Levellier F, Weinbach S, Lahav M, Leiserowitz L, Kjaer K, Als-Nielsen J (1991) Crystal-structures of self-aggregates of insoluble aliphatic amphiphilic molecules at the air–water interface—an X-ray synchrotron study. J Am Chem Soc 113:7684–7691

Janosch S, Nicolini C, Ludolph B, Peters C, Volkert M, Hazlet TL, Gratton E, Waldmann H, Winter R (2004) Partitioning of dual-lipidated peptides into membrane microdomains: lipid sorting versus peptide aggregation. J Am Chem Soc 126:7496–7503

Kaganer VM, Möhwald H, Dutta P (1999) Structure and phase transitions in Langmuir monolayers. Rev Mod Phys 71:779–819

Kjaer K, Als-Nielsen J, Helm CA, Tippmann-Krayer P, Möhwald H (1989) Synchrotron X-ray diffraction and reflection studies of arachidic acid monolayers at the air–water interface. J Phys Chem 93:3200–3206

Malkova S, Long F, Stahelin RV, Pingali SV, Murray D, Cho W, Schlossman ML (2005) X-ray reflectivity studies of cPLA2{alpha}-C2 domains adsorbed onto Langmuir monolayers of SOPC. Biophys J 89:1861–1873

Maltseva E, Brezesinski G (2004) Adsorption of amyloid beta (1–40) peptide to phosphatidylethanolamine monolayers. Chemphyschem 5:1185–1190

McConnell H (2006) Structures and transitions in lipid monolayers at the air–water interface. Ann Rev Phys Chem 42:171–195

Meister A, Nicolini C, Waldmann H, Kuhlmann J, Kerth A, Winter R, Blume A (2006) Insertion of lipidated Ras proteins into lipid monolayers studied by infrared reflection absorption spectroscopy (IRRAS). Biophys J 91:1388–1401

Nagle JF, Tristram-Nagle S (2000) Structure of lipid bilayers. Biochim Biophys Acta 1469:159–195

Nicolini C, Baranski J, Schlummer S, Palomo J, Lumbierres-Burgues M, Kahms M, Kuhlmann J, Sanchez S, Gratton E, Waldmann H, Winter R (2006) Visualizing association of N-Ras in lipid microdomains: influence of domain structure and interfacial adsorption. J Am Chem Soc 128:192–201

Parker MW (1990) A dynamic model of etiology in temporomandibular disorders. J Am Dent Assoc 120:283–290

Pedersen JS, Hamley WI (1994) Analysis of neutron and X-ray reflectivity data. II Constrained least-squares methods. J Appl Cryst 27:36–49

Reuther GW, Der CJ (2000) The Ras branch of small GTPases: Ras family members don't fall far from the tree. Curr Opin Cell Biol 12:157–165

Reuther G, Tan K-T, Köhler J, Nowak C, Pampel A, Arnold K, Kuhlmann J, Waldmann H, Huster D. (2006a) Structural model of the membrane-bound C-terminus of lipid-modified human N-Ras protein. Angew Chem Int Ed Engl 45:5387–5390

Reuther G, Tan K-T, Vogel A, Nowak C, Kuhlmann J, Waldmann H, Huster D (2006b) The lipidated membrane anchor of the N-Ras protein shows an extensive dynamics as revealed by solid-state NMR. J Am Chem Soc 128(42):13840–13846

Schalke M, Lösche M (2000) Structural models of lipid surface monolayers from X-ray and neutron reflectivity measurements. Adv Colloid Interface Sci 88:243–274

Schroeder H, Leventis R, Rex S, Schelhaas M, Nagele E, Waldmann H, Silvius JR (1997) *S*-Acylation and plasma membrane targeting of the farnesylated carboxyl-terminal peptide of N-Ras in mammalian fibroblasts. Biochemistry 36:13102–13109

Seitz HR, Heck M, Hofmann KP, Alt T, Pellaud J, Seelig A (1999) Molecular determinants of the reversible membrane anchorage of the G-protein transducin. Biochemistry 38:7950–7960

Spaar A, Munster C, Salditt T (2004) Conformation of peptides in lipid membranes studied by X-ray grazing incidence scattering. Biophys J 87:396–407

Vogel A, Katzka CP, Waldmann H, Arnold K, Brown MF, Huster D (2005) Lipid modifications of a Ras peptide exhibit altered packing and mobility versus host membrane as detected by (2)H solid-state NMR. J Am Chem Soc 127:12263–12272

Volkert M, Uwai K, Tebbe A, Popkirova B, Wagner M, Kuhlmann J, Waldmann H (2003) Synthesis and biological activity of photoactivatable N-Ras peptides and proteins. J Am Chem Soc 125:12749–12758

Wittinghofer A, Waldmann H (2000) Ras—a molecular switch involved in tumor formation. Angew Chem Int Ed 39:4192–4214